Kinematic Analysis of Powered Lower Limb Orthoses for Gait Rehabilitation of Hemiplegic and Hemiparetic Patients

M. R. Safizadeh, M. Hussein, M. S. Yaacob, M. Z. Md Zain, M. R. Abdullah, M. S. Che Kob, K. Samat

Abstract **-** In this paper, the kinematic analysis of constructed assistive robotic leg for rehabilitation of patients who encounter the neurological injury is presented. In order to design an efficient new mechanism, studies were carried out to distinguish the human architecture and dynamics. In the study, the motion of a healthy physical subject in walking situation of 1 km/h speed was recorded. Thereafter, a novel robotic leg mechanism was developed to produce similar motion. The robotic leg is driven by a single actuator to drive both the hip and the knee joints mechanism. In order to verify the robot motion with respect to human motion, kinematic analysis of all robot's joints and links are formulated and are simulated in MATLAB software. The results obtained from the kinematic analysis of the developed assistive robotic system show that its motion conforms to the motion and dynamics of a healthy human.

Keywords - Kinematic analysis, assistive robotic leg, lower extremity exoskeleton, hemiplegic and hemiparetic patient.

I. INTRODUCTION

The third and seventh causes of death in the world are stroke and accident, respectively. In USA for example, according to the American Heart Association and the National Heart, Lung, and Blood Institute (NHLBI), the cost of tending to people who suffer from cardiovascular diseases and stroke in 2009 is estimated to be $475.3 billion, making stroke a major financial burden to society. This cost includes both direct and indirect costs; direct costs include the cost of physiotherapists and other professionals, hospital and nursing home services, the cost of medications, home health care and other medical durables and indirect costs include lost productivity that results from illness and death. Patients with hemiplegia and palsy may not able to carry out the daily activities such as talking, walking, crouching and grasping; therefore, they need to improve their abilities by active and passive rehabilitation therapy iteratively and regularly. In passive exercises, the patient receive the rehabilitation exercises by physiotherapist; whereas, the active exercises are done by the patients. Unfortunately, although many attempts and researches have been done to prevent the people from accident and death, the number of stroke and injured patients who survive from these events which require rehabilitation services increase with time and also the number of specialists, physiotherapists and rehabilitation centers is not sufficient to respond to a large number of patients efficiently. Thus, after successful presence of robot in industries, the robotic knowledge has been applied in order to carry out the rehabilitant tasks efficiently and less costly. However, medicine and medical doctor must be involved in the development to assure the robot is employed in an ethical way [1].

In recent years, the attention on robotic rehabilitation has been increasing in order to train the patient base on their daily activities. However, because of some disadvantages of medical robots such as neglecting the social and psychological needs of patients, suppression the individuality and uniqueness of services, rejection of autonomous services, and increase of cost, they are not widely applied in medical and rehabilitation centers these days [1]. Hence, researchers have been trying to improve the interaction of robots and their environments and patients in order to carry out some beneficial repetitive exercises.

Indeed, psychological feedback as one of significant step in medical robot design should be taken into account to assess the patients and their performance. Medical robot should be able to record and quantify patient's performance and provide score, statistics, comparisons between normal human and tested patient as well as comparison between new and previous performance to show the patient's progress. In addition, the feedback should able to motivate patients to utilize all their efforts in improvement; also it can inform the user and physiotherapist about movement errors and patients' motion conditions.

As the number of survivors from incidents such as accident, wars and strokes grows, the attention of researchers on developing rehabilitation robots for lower and upper extremity exoskeletons to help hemiplegic patients has been augmented, [2-7, 8]. Professor Sankai in University of Tsukuba for example, has developed a hybrid assistive leg (HAL-3) which assists the disabled in developing normal walking motion. He uses two DC motors

on knee and hip joints, sensory systems in terms of rotary encoder to measure the joints angles, force sensors to measure floor reaction and myoelectricity sensor to estimate the required torques for knee and hip joints and control system [5-6]. However, since the biological signal such as myoelectricity is not estimated for HAL-3 accurately, Suzuki K. et al. proposed two new algorithms in case of floor reaction force (FRF) estimation and torso angle estimation in order to estimate patient's intentions effectively [9]. Professor Kazerooni and his research group carried out extensive research on developing Berkeley lower extremity exoskeleton (BLEEX) in order to help the people to carry significant loads in some situations such as staircases and rocky slopes, in which wheeled vehicles are not able to accomplish these tasks. The developed system highlighted four features which include: a novel control scheme, high-powered compact power supplies, special communication protocol and electronics, and a specific architecture to decrease the complexity and power consumption [10].

Besides, several other designs and methods of actuations have been proposed to provide comfort to patient in walking motion. Artificial pneumatic muscles prototype (KAFO) and (AFO) [11-15], was proposed for knee-ankle-foot orthosis and electro-pneumatic gait orthosis [16]. In addition, electrical actuators for different numbers of DOF [5, 7, 17 and 18] and hydraulic actuators were also designed in order to provide the required force and torque to move the hip, knee and ankle joints correctly [10]. Therapy in case of orthosis with treadmill training has been applied for more than 10 years and has been proven to cure and improve gait of patients. Lokomat Gait Orthosis [19], one of robotic orthosis, utilizes treadmill and body weight support system to handle patient balance. This orthosis assists patient's leg movement using exoskeleton structure support; in addition, hip and knee patient's joints are supported by linear drive actuator that attach to the exoskeleton. Besides the orthosis and exoskeleton with active drivers, some other passive orthosis have been designed in order to exercise patients. For instance, the Spring Brake Orthosis (SBO) has been proposed as a new technique in order to provide hip flexion [20]. The concept of Spring Brake Orthosis, generally, uses potential energy that being stored in the spring to assist torque on the hip flexion. The spring also acts as a knee resistant during knee extension. Other than the function of spring potential energy, a brake is designed to counteract knee flexion and maintain knee extension. This exoskeleton consists of multiple-brake and brake-actuator in order to control rotation of the knee joint. The brake was mounted between shank segments and thigh segments then exactly aligned centrically with the joint axis.

This paper will present the design and kinematic analysis of one DOF lower extremity exoskeleton that moves in parallel to human hip and knee joints in order to train the patient with repetitive physical therapy without considering its ability to climb or walk on the stairs. A low cost, lightweight, simple and accurate mechanism is the main target of the design. It is an exoskeleton powered by a single DC motor that can synchronize the angular position and velocity of the hip and knee joints by means of a gear and cam-follower mechanism. The cam profile is obtained based on the human motion data acquired from joint angles of the lower limbs. The necessary experiments (Fig. 1) are conducted in order to obtain the essential data (Fig. 2).

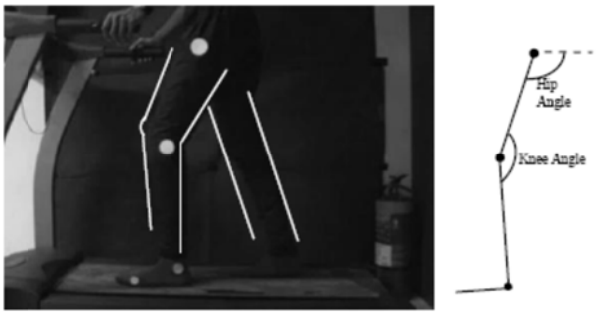

Fig. 1: Captured video in MATLAB MPlay GUI

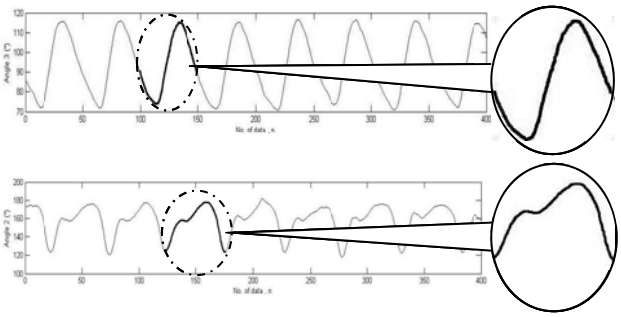

Fig. 2: Experimental Hip (a) and Knee (b) data angles

II DATA ACQUISITION AND MECHANISM DESIGN

In order to design an appropriate robotic leg, the anthropomorphic design contexts were followed, producing two major considerations. The first concern of anthropomorphic design is to make the length of each limb variable to be used for several patients. As the exoskeleton's joints should rotate in the same axis with human joint, any injury or pain to the patient should be avoided. Another major concern is to match the leg kinematic with human motion. This is achieved through the design of a proper drive mechanism with lightweight components, less number of links and lower energy consumptions. Thus, in order to design an anthropomorphic and economic architecture, the two main links with variable length are proposed which can be fastened to the thigh and shin. To have a suitable kinematics of human motion, a mechanism consisting of a DC motor, gears and cam-follower is proposed such that the knee joint motion follows the hip joint angle to make the system a single DOF mechanism as shown in Fig.3.

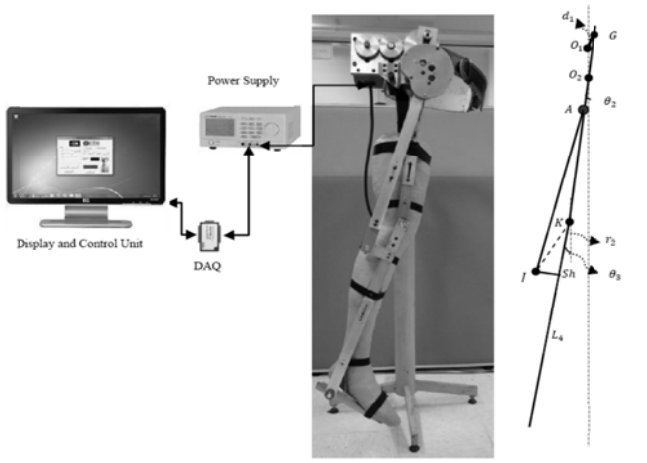

Fig. 3: Block Diagram

A. Cam Design

Since the objective of designing assistive robot is to produce vivid lifelike human motion [21], in the conducted experiment, human motion is captured using Sony DCR-DVD 605 with ability of 25 fps frame rate and are processed by extracting frames out of the video; thereafter. The extracted frames (Fig. 1) are processed as images using MATLAB image processing toolbox. Through image processing at the stage of data acquisition, a total 400 sequential frames are processed for walking speed of 1 km/h. The joint coordinates obtained from image processing are later used to derive joint angles and cam profile based on a single cycle data.

In the design, the hip angle is determined by gear rotation (θ_1), whereas, the knee angle depends on the *link 1* motion as well as cam profile. The accuracy of cam profile therefore contributes to the accuracy of the knee angle motion. Fig. 2 illustrates that the range of angles for hip and knee movement for walking speed of 1 km/h is between 72° to 115° and 126° to 178°, respectively. The angular data from both hip and knee profiles are revised to produce a more practical data thereafter before conversion into follower's linear data which are used to produce the cam profile (*see* Fig. 7).

After designing the robot, the control system hardware and software (driver, transducers, user interface etc.) for controlling the robot motions were developed to accommodate varieties of patient needs; as patient dynamics varies from one to another. The control system software is designed to be user-friendly as such any physiotherapist with simple guides can operate the system. The system can be set for patients of different limb sizes and different rehabilitation exercise speed requirements. Emergency switch is also included to accommodate emergency situations.

III KINEMATIC ANALYSIS

As mentioned earlier, since the powered lower limb orthosis should follow the anthropomorphic and ergonomic design, the kinematic of lower extremity exoskeleton should be proper for human motion. In order to achieve the desirable objective, the kinematic analysis of the power assistive leg is carried out based on simple dynamic relationship and MATLAB programming. The kinematic relationship of the system are acquired on the basis of kinematic analysis of the three links (*link 1* to *link 3*; *see* Fig. 3), cam-follower and relative motion principles [22].

A. Kinematic Analysis of 'link 1'

Since the design and measurement of all links are obtained according to the adaption of human kinematic and lower extremity exoskeleton kinematic, *link 1* follows the thigh's angle with pendulous motion around point O_2. In this design, all measurements such as d_1 and *link 1* slot are acquired from patient's thigh size and the experimental data of hip angle; therefore, the size of 3.1 cm and 39.5 cm are found appropriate for d_1 and *link 1* respectively, as shown in Fig. 3.

In the kinematic analysis, the following assumptions were made:

- The gear movement involves the motion of the rod (d_1).
- Point P is a point on the slot closest to G.
- The rotating axes are assumed to be at *link 1*.

Based on the relative motion of rotating axes, (1) to (3) is introduced to formulate the velocity of one point (such as point P) on *link 1*.

$$V_p = V_{P/G} + V_G \tag{1}$$

$$\begin{cases} V_P - V_G \sin\theta_1 \sin\theta_2 - V_G \cos\theta_1 \cos\theta_2 = 0 \Rightarrow \\ V_P = V_G \cos(\theta_1 - \theta_2) \end{cases} \tag{2}$$

$$\begin{cases} V_{P/G} - V_G \sin\theta_2 \cos\theta_2 + V_G \sin\theta_1 \cos\theta_2 = 0 \Rightarrow \\ V_{P/G} = V_G \sin(\theta_1 - \theta_2) \end{cases} \tag{3}$$

Once the velocity of point P has been acquired, the relationship between angular velocity of *link 1* and angular displacement of the gear (*see* Fig. 5) can be obtained based on (4) below.

$$\omega_2 = \theta_2 = \frac{V_P}{L_1} = \frac{V_G}{L_1}\cos(\theta_1 - \theta_2) \tag{4}$$

where, θ_1 is the angular displacement of the gear, and the relationship between L_1 and θ_2 can be expressed as follows:

$$L_1 = \sqrt{(d_1^2 + d_2^2 - 2d_1 d_2 \cos\theta_1)} \tag{5}$$

$$L_1 \sin\theta_2 = d_1 \sin\theta_1 \Rightarrow \theta_2 = -\sin^{-1}(\frac{d_1}{L_1}\sin\theta_1) \tag{6}$$

Thereafter, the relationship between the absolute velocity of the knee and the angular displacement of the gear as shown in Fig. 6 is obtained from following equation:

$$V_{Knee} = L_2 \omega_2 \quad (7)$$

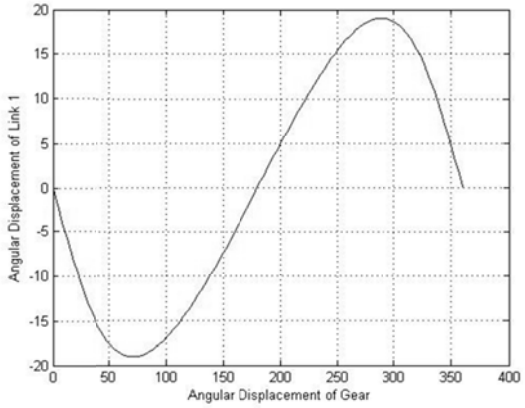

Fig. 4: Angular displacement of *link 1* (θ_2) for one cycle

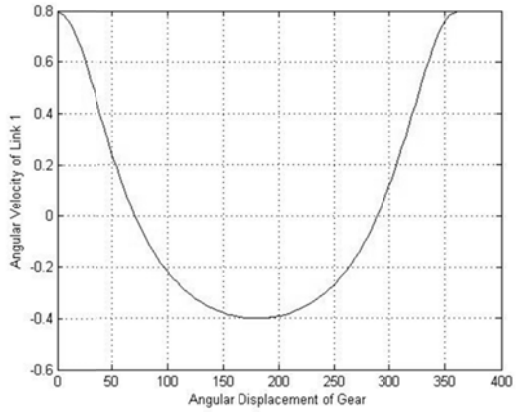

Fig.5: Angular velocity of *link 1* (ω_2) for one cycle

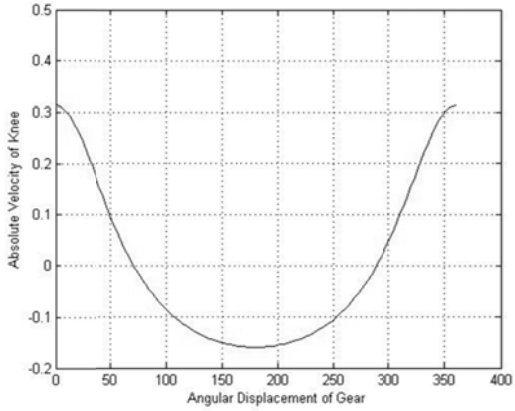

Fig.6: Absolute velocity of knee for one cycle

Because of pendulous motion of *link 1*, the angular velocity of *link 1* as well as the absolute velocity of the knee is in accordance with the pendulous motion with a frequency of 0.26 Hz. Meanwhile, the angular velocity of DC motor is 3.28 rad/s.

B. Kinematic Analysis of 'link 2'

In order to find the angular velocity of the *link 2*, the velocity of roller A; a point on follower has to be obtained. To this end, since the angular velocities for both cam and *link 1* directly affected the velocity of roller, the absolute roller velocity can be found by dividing V_A into two velocities named, V_{A1} and V_{A2}. Velocity V_{A1} and V_{A2} are obtained by assuming the cam is rotating while the link is fixed and the link is rotating while cam is fixed respectively. As indicated earlier, the linear motion data which are used to produce cam profile are shown in Fig. 7.

It can be seen from the graph that the displacement of the follower for rotational link is smoother than the fixed link condition in vertical direction. The profile also shows that there are dwells at the beginning and end as well as in the middle of the cycle. These are important parameters for obtaining smooth motion of the follower. Actually, this comparison is done to illustrate that the data for cam in relation to rotational link is correct and applicable. Hence it produces a smooth motion for the follower and the simulation.

In order to derive the kinematic relationship based on the MATLAB programming, the most correct and proper data should be acquired by interpolating the real cam profile data (Figs. 8 and Fig. 9). As a result, the absolute velocity of roller while the link is assumed fixed (V_{A1}) are demonstrated as shown in Fig.10.

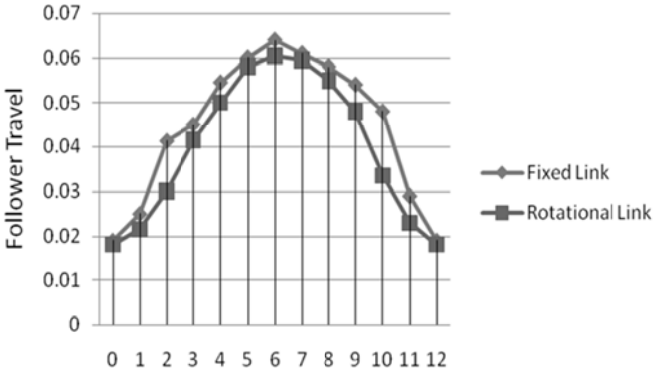

Fig.7: Cam profiles in case of fix and rotational link

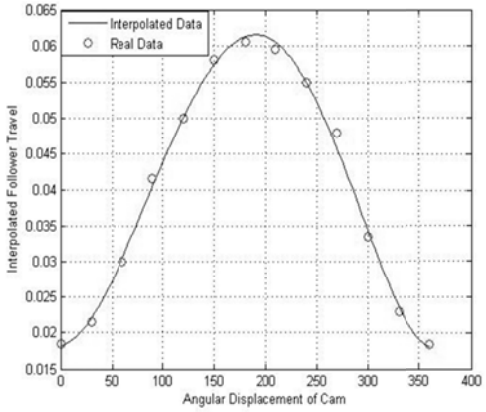

Fig. 8: Interpolated follower displacement and real data for one cycle

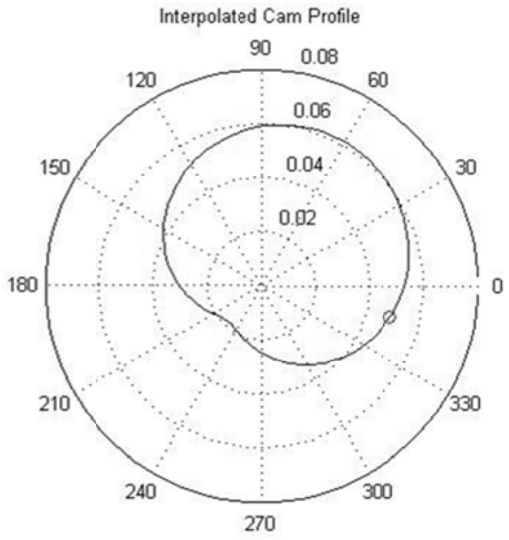

Fig.9: Interpolated cam profile

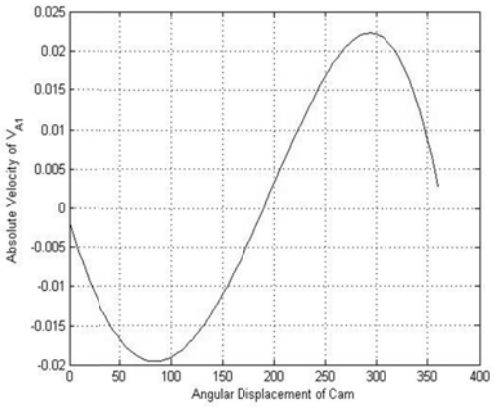

Fig. 10: The absolute velocity of V_{A1} for one cycle

The most complicated part is finding the velocity V_{A2}. The exact position of the roller based on the rotation of the cam (θ_3) and the rod (θ_2) are needed. Subsequently, the tangential vector of cam at this position is required to calculate V_{A2} with its exact direction. Once the absolute velocity of V_{A2} is acquired (as shown in Fig. 11), by analyzing the angular velocity of *link 1* and distance of roller to O_2, and the angle between V_{A1} and V_{A2} (i.e. θ_A), the absolute velocity of the roller, V_A, is obtained based on (8) below. Fig. 12 shows the relationship between the absolute velocity V_A and the gear angular displacement.

$$V_A = \sqrt{V_{1A}^2 + V_{2A}^2 + 2V_{1A}V_{2A}\cos\theta_A} \tag{8}$$

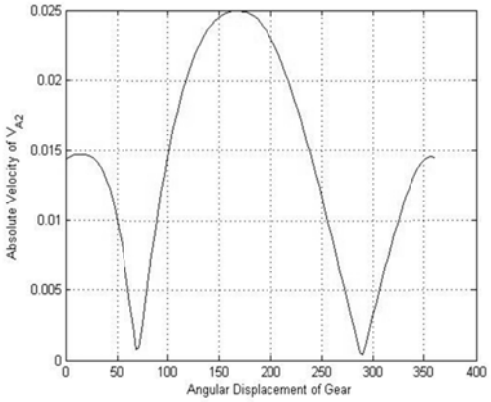

Fig. 11: The absolute velocity of V_{A2} for one cycle

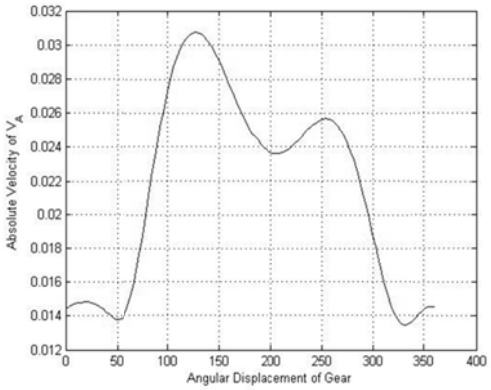

Fig. 12: The absolute velocity of V_A for one cycle

Since the lower part of exoskeleton has general motion and rotates by means of cam-follower mechanism, the angular velocity of *link 2* is acquired by utilizing the absolute velocity of *roller A* and the knee, and the combination of both algebraically and graphically. Consequently, the magnitude of joint *Sh* is generated in respect to the knee joint. On the other hand, the absolute velocity of joint *J* can be found using relative motion analysis with respect to *roller A*.

$$\ddot{V}_{Sh} = \vec{\vec{V}}_K + \dot{\vec{V}}_{Sh/K} \tag{9}$$

$$\ddot{V}_J = \vec{\vec{V}}_A + \dot{\vec{V}}_{J/A} \tag{10}$$

$$\ddot{V}_J = V_{J/Sh} + \ddot{V}_{Sh} \tag{11}$$

Since link *J-Sh* is fixed to *link 2*, the relative velocity of $V_{J/Sh}$ is zero; therefore, (12) is derived from (11) which is shown in vector diagram in Fig. 13 to Fig. 17 for the five cases that follow. Subsequently, the value of $V_{Sh/k}$ and $V_{J/A}$ are acquired based on Figs. 13 to Fig. 17 as well as using (13) through (22).

$$\vec{\vec{V}}_K + \dot{\vec{V}}_{Sh/K} = \vec{\vec{V}}_A + \dot{\vec{V}}_{J/A} \tag{12}$$

Case I ($0° < \theta_1 < \theta_{stop-1}$):

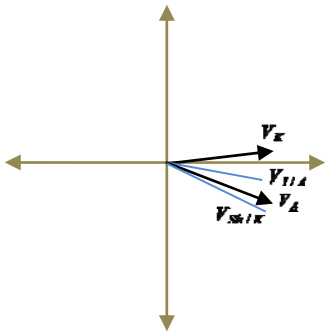

Fig: 13: Velocity vector diagram

Based on the vector diagram in Fig. 13, the vector components in the x and y directions are:

$$x: V_A \sin\theta_A + V_{J/A}\cos\theta_{JA} - V_K\cos\theta_2 - V_{ShK}\cos\theta_{ShK} = 0 \quad (13)$$

$$y: -V_A\cos\theta_A - V_{J/A}\sin\theta_{JA} - V_K\sin\theta_2 + V_{ShK}\sin\theta_{ShK} = 0 \quad (14)$$

Case II ($\theta_{stop-1} < \theta_1 < 180°$):

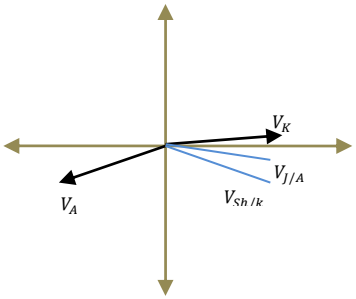

Fig: 14: Velocity vector diagram

$$x: -V_A sin\theta_A + V_{J/A}cos\theta_{JA} + V_K cos\theta_2 - V_{ShK}cos\theta_{ShK} = 0 \quad (15)$$

$$y: -V_A cos\theta_A - V_{J/A}sin\theta_{JA} + V_K sin\theta_2 + V_{ShK}sin\theta_{ShK} = 0 \quad (16)$$

Case III ($180° < \theta_1 < 180° + \theta_{Small}$):

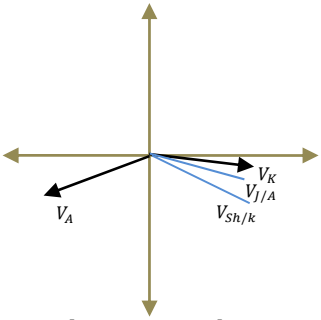

Fig: 15: Velocity vector diagram

$$x: -V_A sin\theta_A + V_{J/A}cos\theta_{JA} + V_K cos\theta_2 - V_{ShK}cos\theta_{ShK} = 0 \quad (17)$$

$$y: -V_A cos\theta_A - V_{J/A}sin\theta_{JA} - V_K sin\theta_2 + V_{ShK}sin\theta_{ShK} = 0 \quad (18)$$

Case IV ($180° + \theta_{Small} < \theta_1 < \theta_{stop-2}$):

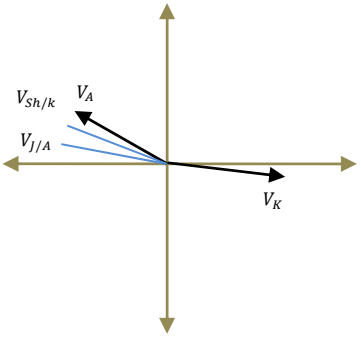

Fig: 16: Velocity vector diagram

$$x: -V_A sin\theta_A - V_{J/A}cos\theta_{JA} + V_K cos\theta_2 + V_{ShK}cos\theta_{ShK} = 0 \quad (19)$$

$$y: -V_A cos\theta_A + V_{J/A}sin\theta_{JA} - V_K sin\theta_2 - V_{ShK}sin\theta_{ShK} = 0 \quad (20)$$

Case V ($\theta_{stop-2} < \theta_1 < 360°$):

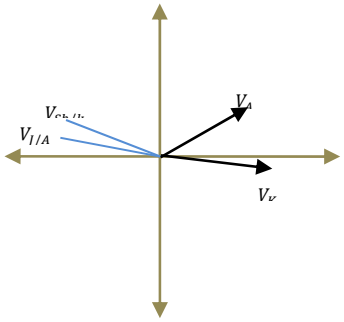

Fig: 17: Velocity vector diagram

$$x: -V_A sin\theta_A - V_{J/A}cos\theta_{JA} - V_K cos\theta_2 + V_{ShK}cos\theta_{ShK} = 0 \quad (21)$$

$$y: -V_A cos\theta_A + V_{J/A}sin\theta_{JA} + V_K sin\theta_2 - V_{ShK}sin\theta_{ShK} = 0 \quad (22)$$

Since the magnitudes of V_K and V_A are computed from (7) and (8), the values and direction of $V_{Sh/K}$ and $V_{J/A}$ are obtained using (12) and the known angular position of *link 1* (θ_2) and θ_A. The angular velocities of *link 2* and *link 3* can be found by analyzing the relative velocities of $V_{Sh/K}$ and $V_{J/A}$. Once the angular velocity of *link 2* is calculated, the relative velocity $V_{Bot/K}$ can be obtained using (23) below.

$$V_{bot/K} = \frac{L_4}{r_2} V_{Sh/K} \tag{23}$$

Since of $V_{Bot/K}$ can be found, the magnitude as well as the direction of ankle velocity are obtained based on (24) through (27).

$$V_B = V_{B/K} + V_K \tag{24}$$

$$V_A = \sqrt{V_K^2 + V_{B/K}^2 + 2V_K V_{B/K} \cos(\theta_2 + \theta_{Sh/K})} \tag{25}$$

In addition, the angle between V_k and V_B for different cases is obtained, using (18) with respect to Fig. 18 to Fig. 22 in which also provide the direction of V_B for each cases.

$$\theta_{B-K} = \cos^{-1}\left(\frac{V_B^2 + V_K^2 - V_{B/K}^2}{2 \times V_B \times V_K}\right) \tag{26}$$

It can be seen from the figures that the value of θ_B depends on the configuration of V_B, V_k and $V_{B/k}$ for the respective cases.

Case I ($0° < \theta_1 < \theta_{stop-1}$):

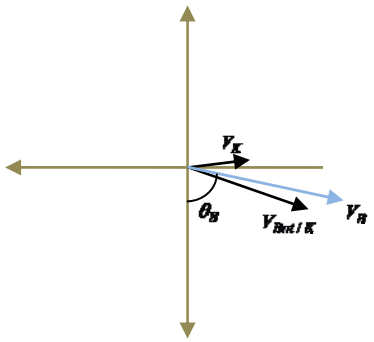

Fig. 18: Velocity vector diagram

$$\theta_B = -[90 - (\theta_{B-K} - |\theta_2|)] \tag{27}$$

Case II ($\theta_{stop-1} < \theta_1 < 180°$):

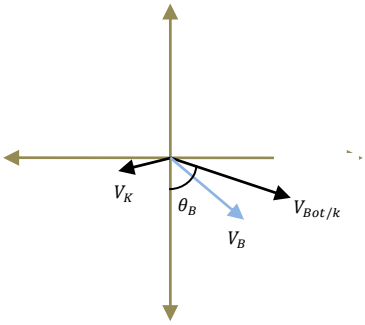

Fig. 19: Velocity vector diagram

$$\theta_B = -[\theta_{B-K} - (90 - |\theta_2|)] \tag{28}$$

Case III ($180° < \theta_1 < 180° + \theta_{Small}$):

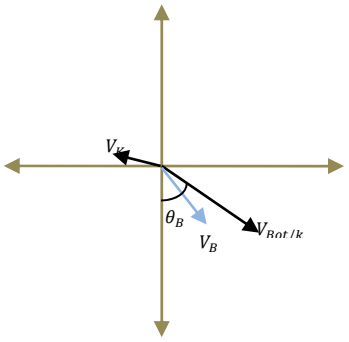

Fig. 20: Velocity vector diagram

$$\theta_B = -[(\theta_{B-K} - |\theta_2|) - 90] \tag{29}$$

Case IV ($180° + \theta_{Small} < \theta_1 < \theta_{stop-2}$):

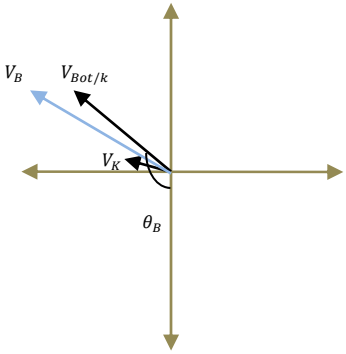

Fig. 21: Velocity vector diagram

$$\theta_B = [(\theta_{B-K} + |\theta_2|) + 90] \tag{30}$$

Case V ($\theta_{stop-2} < \theta_1 < 360°$):

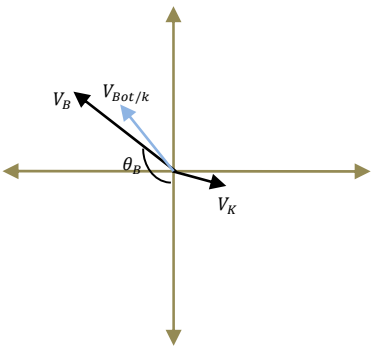

Fig. 22: Velocity vector diagram

$$\theta_B = [(90 - |\theta_2|) + \theta_{B-K}] \tag{31}$$

Comparing Fig. 24 with Fig. 2(a), and Fig. 25 with Fig. 2(b), the simulation data acquired based on kinematic analysis show good agreement with the simulation results obtained from the MATLAB programming.

In order to calculate the step size for the robotic leg, it is assumed that in each step the fore foot is vertical to the ground, and rear foot hip angle is at maximum position (17°) (*see* Fig. 26). Thus, the step size (d_{Step}) is calculated on the basis of known values for the link length and the hip maximum angle.

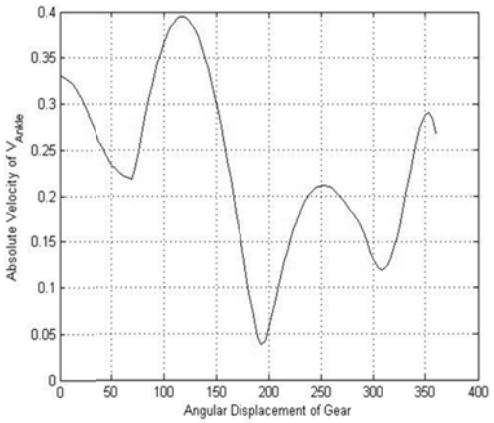

Fig. 23: Definitive absolute velocity of V_{Ankle} for one cycle

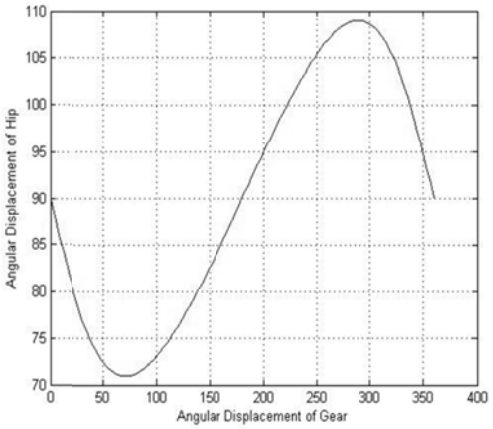

Fig. 24: Definitive angular position of hip for one cycle

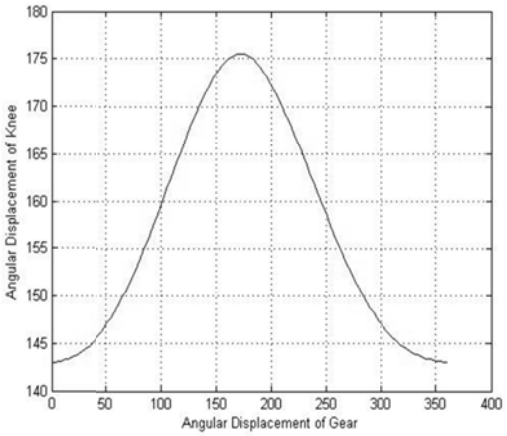

Fig. 25: Definitive angular position of knee for one *cycle*

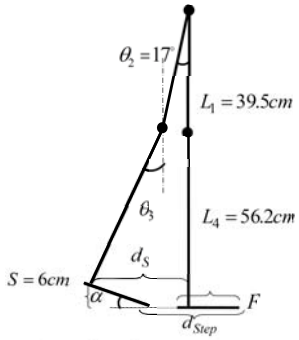

Fig. 26: Human step size during each stage of the gait

Trigonometric and geometric relationships are shown in the following equations:

$$L_1 \times \cos\theta_2 + L_4 \times \cos\theta_3 + S = L_1 + L_4 \Rightarrow \theta_3 = 24.69^\circ \quad (32)$$

$$d_S = L_1 \times \sin\theta_2 + L_4 \times \sin\theta_3 \Rightarrow d_S = 31cm \quad (33)$$

$$d_{Step} = d_S - F \times \sin\alpha + F \Rightarrow d_{Step} = 53cm \quad (34)$$

Therefore, the patient gait through a distance is $2 \times d_{Step} = 106cm$ in each cycle which is accordance with human step's length and within the patient's ability.

IV. CONCLUSION

This paper presents an assistive robotic leg (lower extremity exoskeleton) which was designed and developed based on acquired experimental walking data in order to help to train the stroke sufferers. The experimental hip and knee angles for 1 km/h walking speed were obtained by using MATLAB image processing toolbox. Thereafter, the angular data was converted to linear motion in order to design a proper cam-follower mechanism. In this work, a significant deference between the present prototype and previous designs is that the design and development of lower extremity exoskeleton mechanism using only a single DC motor to control the movement of both the hip and the knee joints. In the end, the kinematic analysis and simulation were carried out based on the proposed design. The kinematic results were compared with the experimental data to prove its validity. The validated simulation data obtained from the kinematic analysis are very useful and will be applied in future studies.

ACKNOWLEDGMENT

The authors would like to thank the Malaysian Ministry of Science, Technology and Innovation (MOSTI) and Universiti Teknologi Malaysia (UTM) for their continuous support in the research work. This work was financial supported in part by the Malaysia eSciences Fund under grant number Vot. 79338.

REFERENCES

[1] Liliana Rogozea, Florin Leasu, Angelu Repanovici, Michaela Baritz, Ethics, robotics and medicine development, *Proceedings of the 9th WSEAS international conference on Signal processing, robotics and automation, Robotics and Automation*, 2010, pp. 264-268, ISSN: 1790-5117.

[2] Daniela Mariana Barbu, Ion Barbu, "Dynamical Model for an Original Mechatronical Rehabilitation System, *Proceedings of the 14th WSEAS International Conference on Applied mathematics*, 2009, pp. 23–28, ISSN: 1790-276.

[3] Kao, P.C, Motor adaptation during dorsiflexion-assisted walking with a powered orthosis, *Journal of Gait and Posture*, vol. 29, pp. 230–236, 2009.

[4] Sawicki, G. S., Domingo, A. & Ferris, D. P, The Effects of Powered Ankle-Foot Orthoses on Joint Kinematics and Muscle Activation During Walking in Individuals With Incomplete spinal cord injury, *Journal of Neuro Engineering and Rehabilitation*, vol. 3, pp. 1-17, 2006.

[5] Kawamoto, H. & Sankai, Y., Power Assist System HAL-3 for Gait Disorder Person, in Computers Helping People with Special Needs. *Vol. 2398/2002, ed Heidelberg: Springer Berlin*, 2002, pp. 19-29.

[6] Kawainoto, H., Lee, S., Kanbe, S. & Sankai, Y., Power Assist Method for HAL-3 Using EMG-Based Feedback Controller, *in Proceedings of the IEEE International Conference on Systems, Man, and Cybernetics*, 2003, pp. 1648–1653.

[7] Banala, S. K., Kulpe, A. & Agrawal, S. K., A Powered Leg Orthosis for Gait Rehabilitation of Motor-Impaired Patients, *in IEEE International Conference on Robotics and Automation, Roma, Italy*, 2007, pp. 4140-4145.

[8] Hussein A. Abduallah, Cole Tarry, Mohamed Abderrahim, Robotic Techniques for Upper Limb Rehabilitation and Evaluation, *Proceedings of the 2nd WSEAS International Conference on Dynamical Systems and Control, Bucharest, Romania, 2006, pp. 78-83.*

[9] Kenta, S., Gouji, M., Hiroaki, K., Yasuhisa, H. & Yoshiyuki, S., Intention-Based Walking Support for Paraplegia Patients with Robot Suit HAL, *Journal of Advanced Robotics*, vol. 29, pp. 1441-1469, 2007.

[10] Zoss, A., Kazerooni & Chu, A., On the Mechanical Design of the Berkeley Lower Extremity Exoskeleton (BLEEX), *in IEEE/RSJ International Conference on Intelligent Robots and Systems*, 2005, pp. 3132-3139.

[11] Ferris, D. P., Gordon, K. E., Sawicki, G. S. & Peethambaran, A., An Improved Powered Ankle–Foot Orthosis Using Proportional Myoelectric Control, *Journal of Gait and Posture*, vol. 23, pp. 425-428, 2005.

[12] Ferris, D. P., Sawicki, G. S. & Domingo, A., Powered lower limb orthoses for gait rehabilitation, *Top Spinal Cord International journal of Rehabilitation*, vol. 11, pp. 34-39, 2005.

[13] Gordona, K. E., Sawicki, G. S. & Ferrisa, D. P., Mechanical Performance of Artificial Pneumatic Muscles to Power an Ankle–Foot Orthosis, *Journal of Biomechanics*, vol. 39, pp. 1832-1841, 2006.

[14] G. S. Sawicki and D. P. Ferris, A Pneumatically Powered Knee-Ankle-Foot orthosis (KAFO) With Myoelectric Activation and Inhibition, *Journal of NeuroEngineering and Rehabilitation*, vol. 6, pp. 1-16, 2009.

[15] Sawicki, G. S., Gordon, K. E. & Ferris, D. P., Powered Lower Limb Orthoses: Applications in Motor Adaptation and Rehabilitation, *in 9th International Conference on Rehabilitation Robotics, Chicago, IL, USA*, 2005, pp. 206-211.

[16] Belforte, G., Gastaldi, L. & Sorli, M., "Pneumatic Active Gait Orthosis," Journal of Mechatronics, vol. 11, pp. 301-323, 2001.

[17] Ruthenberg, B. J., Wasylewski, N. A. & Beard, J. E., An Experimental Device for Investigating the Force and Power Requirements of a Powered Gait Orthosis, *Journal of Rehabilitation Research and Development*, vol. 34, pp. 203-213, 1997.

[18] Jerry, E. P., Benjamin, T. K. & Christopher, J. M., The Roboknee: An Exoskleton for Enhancing Strength and Enharance During Walking, *in International Conference on Robotic & Automation, New Orleans*, 2004, pp. 2430-2435.

[19] Gery Colombo, Matthias Joerg, Reinhard Schreier, BNIE, Volker Dietz, Treadmill training of paraplegic patients using a robotic orthosis, *Journal of Rehabilitation Research and Development*, Vol. 37, No. 6, 2000, pp. 693-700.

[20] S. Gharooni, B. Heller, and M. O. Tokhi, A New Hybrid Spring Brake Orthosis for Controlling Hip and Knee Flexion in the Swing Phase, *IEEE Trans Neural System and Rehabilitation Engineering*, Vol. 9, No.1, 2001, pp: 106-107.

[21] J. Kang, B. Badi, Y. Zhao and D. K. Wright, Human Motion Modeling and Simulation**,** *Proceedings of the 6th WSEAS International Conference on Robotics, Control and Manufacturing Technology, Hangzhou, China*, April 16-18, 2006, pp: 62-67.

[22] Meriam, J. L., Kraige, L. G. & Palm, W. J., Engineering Mechanics: *Dynamics, 5 ed.: John Wiley*, 2001.